Materials Letters 158 (2015) 237–240

Contents lists available at ScienceDirect

Materials Letters

journal homepage: www.elsevier.com/locate/matlet

Interconnected mesoporous carbon sheet for supercapacitors from low-cost resources

Xiaoting Wang [a,b], Hao Ma [b], Hebao Zhang [b], Moxin Yu [b], Xiaojun He [b,*], Yong Wang [a,**]

[a] State Key Lab of Materials-Oriented Chemical Engineering, College of Chemistry and Chemical Engineering, Nanjing Tech University, Nanjing 210009, China
[b] School of Chemistry and Chemical Engineering, Anhui University of Technology, 59 Hudong Road, Maanshan 243002, China

ARTICLE INFO

Article history:
Received 29 March 2015
Received in revised form
14 May 2015
Accepted 31 May 2015
Available online 9 June 2015

Keywords:
Porous materials
Carbon materials
Mesoporous carbon sheet
Supercapacitor

ABSTRACT

Interconnected mesoporous carbon sheets (MCSs) were prepared from cheap coal tar pitch with low-cost $CaCO_3$ nanoparticles and cetyltrimethyl ammonium bromide (CTAB) as porogens for supercapacitors. The results show that the surface area of MCSs can be tuned in the range of 87–167 $m^2 g^{-1}$. The interconnected MCS_{2-1-1} made at 2:1:1 of $CaCO_3$/coal tar pitch/CTAB mass ratio retains a capacitance of 87 $F g^{-1}$ at 0.1 $A g^{-1}$ after 100 cycles in ionic liquid electrolyte with high retention of 93.1%, showing excellent cycle stability. The energy density of MCS_{2-1-1} capacitor only drops from 64.18 Wh kg^{-1} to 22.19 Wh kg^{-1} with the average power density increasing from 115 W kg^{-1} to 4267 W kg^{-1}, demonstrating good rate performance. This work suggests a low-cost way to synthesize high performance MCS for energy storage materials.

1. Introduction

Supercapacitors have attracted much attention as the promising energy storage device. Porous carbons including microporous carbon, mesoporous carbon and macroporous carbon, are the main electrode materials for supercapacitors due to their high surface area and good conductivity [1,2]. Aqueous [2] and organic electrolytes [1] as well as ionic liquids [3] are the main electrolytes used in supercapacitors. Ionic liquids show potential applications due to their high decomposition voltage (V) because the energy density of supercapacitor (E) is based on $E=0.5CV^2$. Nevertheless, the energy density of supercapacitors fabricated from microporous carbons obviously decreases at higher current density because of the longer and narrower channels in microporous carbons for the bigger size of electrolyte ions [4,5]. As such, it is of great interest to synthesize mesoporous carbon sheets (MCSs) with shorter and wider channels by using templates or porogens coupled with KOH activation [6]. Nanostructured carbon materials, for example, graphene [7,8] and carbon nanotubes, are also used to prepare supercapacitors, however, they are suffering high costs. Therefore, it is highly desirable to prepare MCS electrode materials for supercapacitors from low-cost resources. In this work, we prepare interconnected MCS for supercapacitors by using low-cost materials as both carbon precursors and porogens. Coal tar pitch is used as carbon precursor for this aim because it is thermoplastic with high carbon yield and low ash content [5]. $CaCO_3$ nanoparticles were selected as templates and porogens because they could be removed easily by diluted acidic solutions. Additionally, a surfactant, cetyltrimethyl ammonium bromide (CTAB) was also used in the synthesis of MCS to improve the dispersibility of $CaCO_3$ nanoparticles and simultaneously functions as a co-porogen to generate additional micropores and mesopores in the carbonization step.

2. Experimental

A coal tar pitch with a softening point of 110 °C provided by Maanshan iron & steel Co., Ltd, was used as the carbon precursor [9]. First, coal tar pitch with a particle size below 100 μm, $CaCO_3$ nanoparticles (ca. 50–100 nm in size from Ruicheng Xintai Nano-Materials Technology Co., Ltd), and CTAB (99.0%) were dispersed in tetrahydrofuran (THF, 99.0%) solution and ethanol solution, respectively. The mixed solution was dried in water bath at 90 °C, and then was transferred to a corundum crucible. The corundum crucible was heated at 5 °C min^{-1} to 850 °C, then kept at 850 °C for 1 h in flowing nitrogen (99.999%). After cooling down to room temperature, the obtained sample was washed with 2 M HCl solution and distilled water thoroughly, then dried at 110 °C for 24 h. The as-made carbon is denoted as MCS_{x-y-z}, where the subscript x, y and z stand for the mass ratio of $CaCO_3$, coal tar pitch and CTAB. The pore structure of MCS was analyzed by the nitrogen adsorption–desorption isotherms at −196 °C (Micrometrics, ASAP 2010)

* Corresponding author. Fax: +86 555 2311822.
** Corresponding author.
E-mail addresses: xjhe@ahut.edu.cn (X. He), yongwang@njtech.edu.cn (Y. Wang).

http://dx.doi.org/10.1016/j.matlet.2015.05.157
0167-577X/

[9]. The microstructures of MCSs and $CaCO_3$ were characterized by field emission scanning electron microscopy (FESEM, Nanosem430), transmission electron microscopy (TEM, JEOL-2100), and X-ray diffraction (XRD, Philips X, CuKa Radiation). The electrodes were prepared by mixing MCS, poly(tetrafluoroethylene) and carbon black in a mass ratio of 89:6:5, and pressed at 15.0 MPa for 10 s, then dried at 110 °C for 1 h under vacuum conditions. More details can be found elsewhere [9]. Button-type supercapacitors were assembled with two similar carbon electrodes separated by a separator in 1-butyl 3-methyl imidazole six fluoride phosphate ($BMIMPF_6$) electrolyte in an Ar-filled glove box. The galvanostatic charge/discharge performance of supercapacitors was evaluated on a land cell tester (CT-2001A) at room temperature.

3. Results and discussion

The nitrogen adsorption–desorption isotherms of the as-made MCSs are shown in Fig. 1(a), which indicate that all of the MCSs contain a number of mesopores and macropores as evidenced by the hysteresis loop [10]. Fig. 1(b) shows that MCS_{2-1-1} possesses the continuous distribution pores, ranging from 25 to 150 nm. MCS_{2-1-2} and MCS_{1-1-1} also has wide distribution pores,

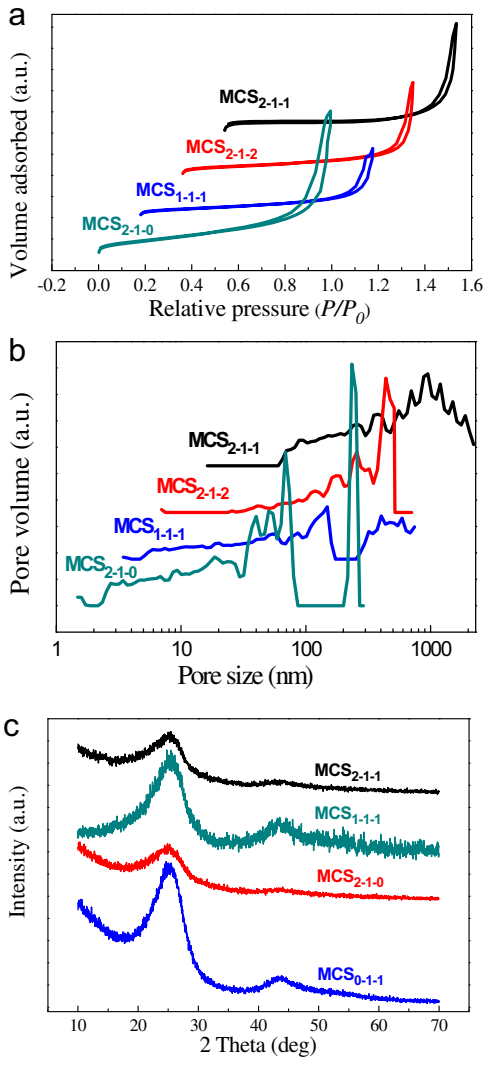

Fig. 1. (a) Nitrogen adsorption–desorption isotherms and (b) pore size distribution of MCSs. (c) XRD patterns of MCSs.

Table 1
Pore structure parameters and yields of MCSs.

MCSs	D_{ap} (nm)	S_{BET} ($m^2\ g^{-1}$)	V_t ($cm^3\ g^{-1}$)	V_{mic} ($cm^3\ g^{-1}$)	Yields (%)
MCS_{2-1-1}	6.71	129	0.22	0.04	11.7
MCS_{2-1-2}	7.21	98	0.18	0.02	11.6
MCS_{1-1-1}	7.00	87	0.15	0.01	19.2
MCS_{2-1-0}	8.90	167	0.37	0.02	43.9

respectively. Yet, the pores of MCS_{2-1-0} center at 19–69 nm and 234–256 nm. The above results show that the pore size can be adjusted by the addition of CTAB to the reactants. Fig. 1(c) shows the XRD patterns of MCS samples. The diffraction peaks at ca. 25–28° and 40–45° are (002) and (100) peaks of MCSs, respectively. The interlayer spacing (d_{002}), the average crystallite size along the *c*-axis (L_c) and the size of the layer planes (L_a) of MCSs were calculated using Bragg's equation and the Scherrer equation, respectively [11]. The L_c and L_a of MCS_{2-1-2} reaches 123 nm and 48 nm, which is the biggest among all the MCSs, respectively. Correspondingly, the d_{002} of MCS_{2-1-2} is 0.349 nm while that of the other three samples ranges from 0.350 nm to 0.358 nm, which are bigger than that of graphite (d_{002}=0.335 nm). The higher d_{002} value means that the MCSs were disordered and proper graphitization had not taken place.

The pore structure parameters of MCSs are summarized in Table 1. Compared to MCS_{2-1-1}, the S_{BET} and V_t of the MCSs drops with decreasing $CaCO_3$ content or increasing CTAB content in the mixture. The S_{BET} of MCS_{2-1-1} is 129 $m^2\ g^{-1}$ with a D_{ap} of 6.71 nm, a V_t of 0.22 $cm^3\ g^{-1}$ and a yield of 11.7%.

Fig. 2(a) and (c) shows the TEM images of the $CaCO_3$ nanoparticles and MCS_{2-1-1}. Fig. 2(a) shows that the diameters of the $CaCO_3$ templates are ca. 50–100 nm (circled by white circles). Fig. 2 (b) shows that the pore sizes of MCS_{2-1-1} are ca. 100 nm, which are formed due to the site-occupation of $CaCO_3$ particles in the precursor matrix. Fig. 2(c) proves that the thin sheets in MCS are interconnected, and a macropore can be seen after $CaCO_3$ particle is removed. Compared to the bigger pore sizes of MCS_{2-1-0} in Fig. 2 (d), Fig. 2(b) illustrates that the pore sizes of MCS_{2-1-1} can be decreased by adding CTAB to the reactants, which is consistent with the variation of the D_{ap} in Table 1.

Fig. 3(a) is the charge–discharge curves of MCS electrodes in $BMIMPF_6$ electrolyte at 0.05 A g^{-1}, which demonstrates that the MCS electrodes have the typical capacitive behavior. Fig. 3 (b) shows the variation of the specific capacitance of MCS electrodes with the current density. The specific capacitance of MCS_{2-1-1} electrode only drops from 117 to 63 F g^{-1} with the current density increasing from 0.05 to 2.0 A g^{-1} because the thin sheet significantly shortens the electrolyte ion diffusion length and the interconnected sheets offer effective electron transport pathways. The surface area-normalized capacitance of MCS_{2-1-1} reaches 90.7 μF cm^{-2} at 0.05 A g^{-1}, and 48.8 μF cm^{-2} at 2 A g^{-1} in $BMIMPF_6$ electrolyte, which is even larger than that of 3D hollow porous graphene ball electrode in 6 M KOH electrolyte [9]. The capacitance of MCS_{2-1-1} is always higher than that of other three electrodes due to its continuous distribution pores. The variation of energy density of MCS capacitors with the average power density is shown in Fig. 3(c). The energy densities of MCS_{2-1-1} capacitor are obviously higher than those of other electrodes. At an average power density of 115 W kg^{-1}, the energy density of MCS_{2-1-1} capacitor is 64.18 Wh kg^{-1}, and remains 22.19 Wh kg^{-1} at 4267 W kg^{-1}, being the highest among all the MCS capacitors and still obviously higher than that of Ru/mesoporous carbon composites in 6 M KOH electrolyte [12]. The variation of the specific capacitance with the cycle number at 0.1 A g^{-1} current density is

shown in Fig. 3(d). After 90 cycles, the capacitance of all the MCS electrodes almost remain the same, and that of MCS_{2-1-1} reaches 93.1% after 100 cycles, displaying excellent cycle stability. The results prove that the MCS made from coal tar pitch using $CaCO_3$ and CTAB as porogens is a low-cost and efficient approach for the production of high performance MCS electrode materials for supercapacitors.

4. Conclusions

Interconnected MCSs for supercapacitors were prepared from low-cost resources with coal tar pitch as carbon precursors by using $CaCO_3$ and CTAB as porogens. The MCS retains a capacitance of 87 F g^{-1} at 0.1 A g^{-1} after 100 cycles in ionic liquid electrolyte with 93.1% capacitance retention, exhibiting excellent cycle

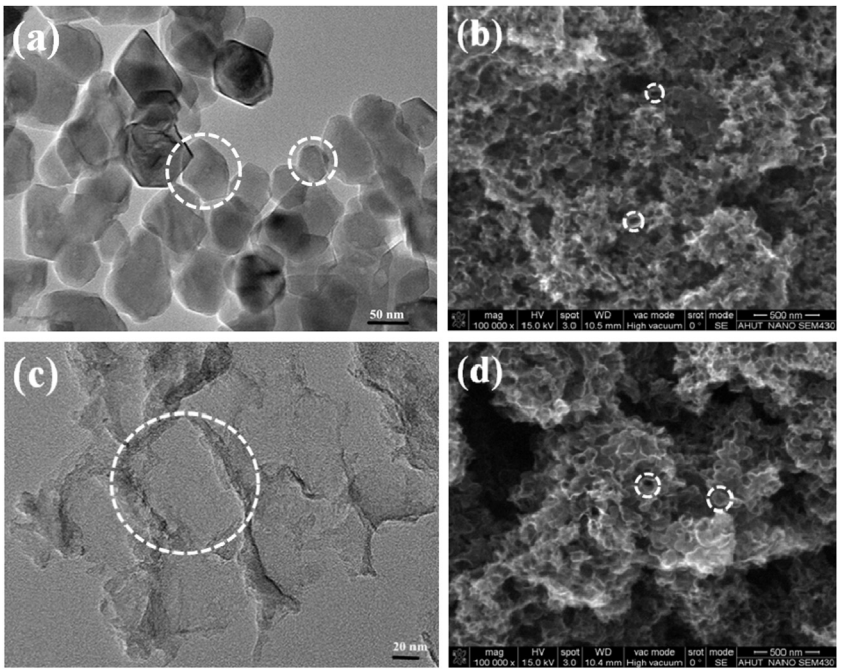

Fig. 2. (a) TEM image of $CaCO_3$ nanoparticles, (b) FESEM image of MCS_{2-1-1}, (c) TEM image of MCS_{2-1-1}, (d) FESEM image of MCS_{2-1-0}.

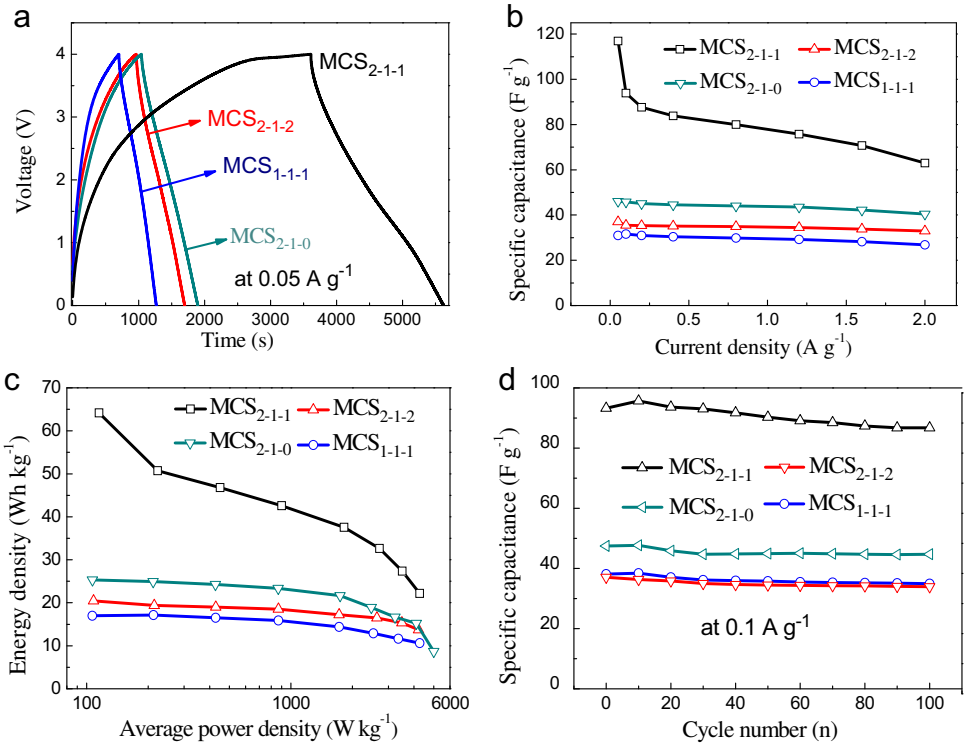

Fig. 3. (a) Galvanostatic charge–discharge curves of MCS electrodes, (b) specific capacitance of MCS electrodes at different current densities, (c) ragone plots of MCS supercapacitors, (d) specific capacitances of MCS electrodes vs. cycle number.

stability. The supercapacitor fabricated from MCS_{2-1-1} shows good rate performance and high surface area-normalized capacitance. This method suggests a low-cost route to synthesize MCS for energy storage materials.

Acknowledgments

This work is supported by the National Natural Science Foundation of China (Nos. 51272004 and U1361110) and the program for new century excellent talents of the State Ministry of Education in China (No. NCET-13-0643).

References

[1] Y.R. Liang, F.X. Liang, H. Zhong, Z.H. Li, R.W. Fu, D.C. Wu, et al., J. Mater. Chem. A 1 (2013) 7000–7005.
[2] M.R. Lukatskaya, O. Mashtalir, C.E. Ren, Y.D. Agnese, P. Rozier, P.L. Taberna, et al., Science 341 (2013) 1502–1505.
[3] M. Galinski, K. Babeł, K. Jurewicz, J. Power Sources 228 (2013) 83–88.
[4] W.F. Zhang, Z.H. Huang, Z. Guo, C. Li, F.Y. Kang, Mater. Lett. 64 (2010) 1868–1870.
[5] X.J. He, N. Zhao, J.S. Qiu, N. Xiao, M.X. Yu, C. Yu, et al., J. Mater. Chem. A 1 (2013) 9440–9448.
[6] W. Lin, B. Xu, L. Liu, New J. Chem. 38 (2014) 5509–5514.
[7] H.Y. Mi, J.P. Zhou, Q.X. Cui, Z.B. Zhao, C. Yu, X.Z. Wang, et al., Carbon 80 (2014) 799–807.
[8] Q.L. Hao, X.F. Xia, W. Lei, W.J. Wang, J.S. Qiu, Carbon 81 (2015) 552–563.
[9] X.J. He, H.B. Zhang, H. Zhang, X.J. Li, N. Xiao, J.S. Qiu, J. Mater. Chem. A 2 (2014) 19633–19640.
[10] B. Xu, S.S. Hou, F.L. Zhang, G.P. Cao, M. Chu, Y.S. Yang, J. Electroanal. Chem. 712 (2014) 146–150.
[11] L. Muniandy, F. Adam, R.A. Mohamed, E. Ng, Microporous Mesoporous Mater. 197 (2014) 316–323.
[12] X.J. He, K. Xie, R.C. Li, M.B. Wu, Mater. Lett. 115 (2014) 96–99.